characteristics that it was about 5 MHz wide at –3 dB, did not appear to be connected with the external circuit parameters, and was present whenever the beam was present in the tube (independent of rf generation at 110 GHz).

Several direct measures were undertaken on the gyrotron in an attempt to reduce the amplitude of this parasite. A capacitive filter, Fig. 7, was connected across the gyrotron accelerating gap. This filter provided a 1 nF short across the tube insulator, with uniform electric field gradient maintained by a voltage divider chain. An iron collar was installed at the top of the tube insulator to eliminate the possibility of a magnetic well with a trapped electron population below the cathode, which might be causing the parasite. The actual effect produced by this collar was to eliminate small internal gyrotron sparks which had been observed during operation in the presence of the parasite, however its effect on the parasite itself was minimal. Additional work on understanding the parasite is in progress [6].

The tube filter installation resulted in a substantial change in the character of the instability. The new spectrum has a small peak at 4.7 MHz with a satellite at 5.7 MHz, plus a strong peak at 96 MHz with sidebands and structure between 88 and 106 MHz. Harmonics out to the third are observed. The 96 MHz peak had not been observed before the installation of the gyrotron filter. The rf spectrum, estimated to have a total power of several kW, is shown in Fig. 8.

This parasite is still observed during normal operation of the gyrotron. There has not been any evidence that the amplitude of the parasite has decreased during the course of gyrotron operation to date. Despite the installation of the tube filters, it continued to be impossible to run the gyrotron without spurious interlock trips and other control and monitoring problems. Therefore a comprehensive program of rf interference suppression, both in the gyrotron system and in other DIII–D systems, was undertaken, which enabled operation in the presence of the parasite.

It has occasionally happened that during normal gyrotron operation the parasite suddenly has become more severe. Reducing the gun coil current by about 10% has permitted return to normal operation and following conditioning the normal operating regime can be restored. The present situation is that the parasite is a serious but generally manageable problem.

V. INITIAL OPERATION INTO DIII–D

Although thus far experimental time has been limited, the gyrotron and transmission line system have been operated into DIII-D plasmas and the principal features of the systems have been checked. The launcher injects the rf power at a fixed angle of 19 degrees off perpendicular to the toroidal field and can be scanned poloidally, as indicated in Fig. 9. Calculations of the spot size in the plasma predict that 98% of the rf power will be distributed across an area

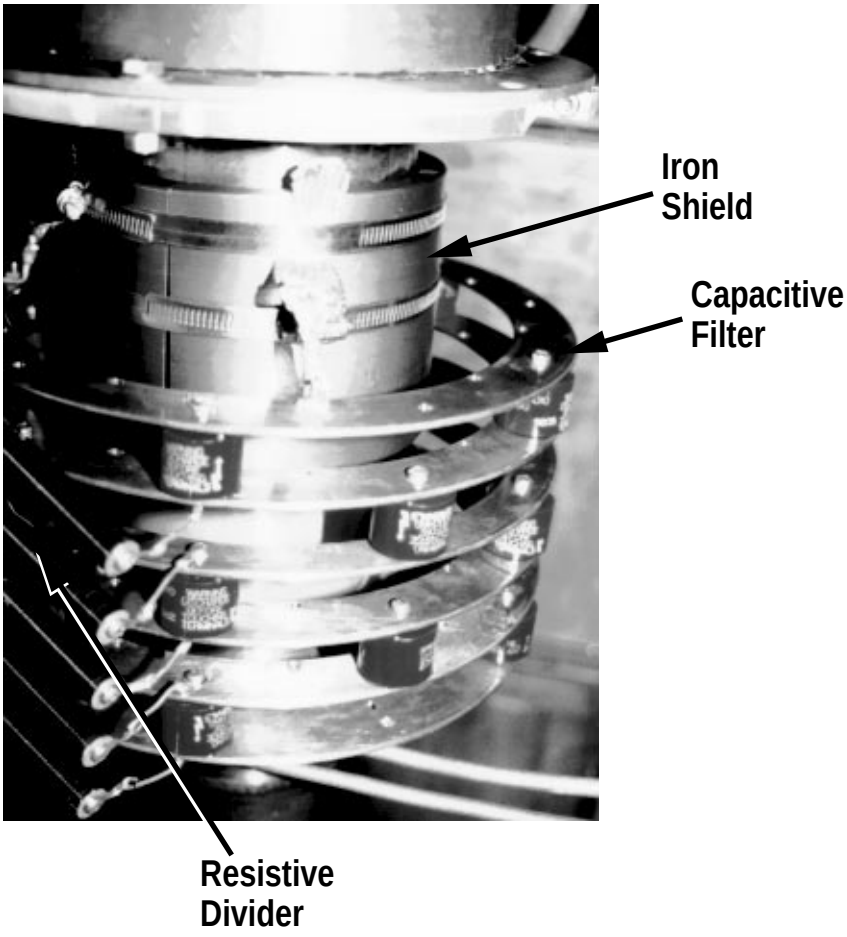

Fig 7. Photograph of the capacitive filter and magnetic collar mounted on the gyrotron inside the high voltage tank. Five planes connected with 5 nF are arranged in series for a total 1 nF filter. The iron collar is mounted on the upper, anode, portion of the gyrotron.

with diameter 12.8 cm at a distance of 1.00 m from the final poloidally scanning mirror. The calculated spot size increases to 16.3 cm diameter at a distance of 1.25 m from the final mirror. The actual power deposition profile was estimated from the change in the time derivative in the ECE T_e signals at the termination of the rf pulse. These measurements are summarized in Fig. 10, where the power deposition profile is seen to be broader than expected and with substantial

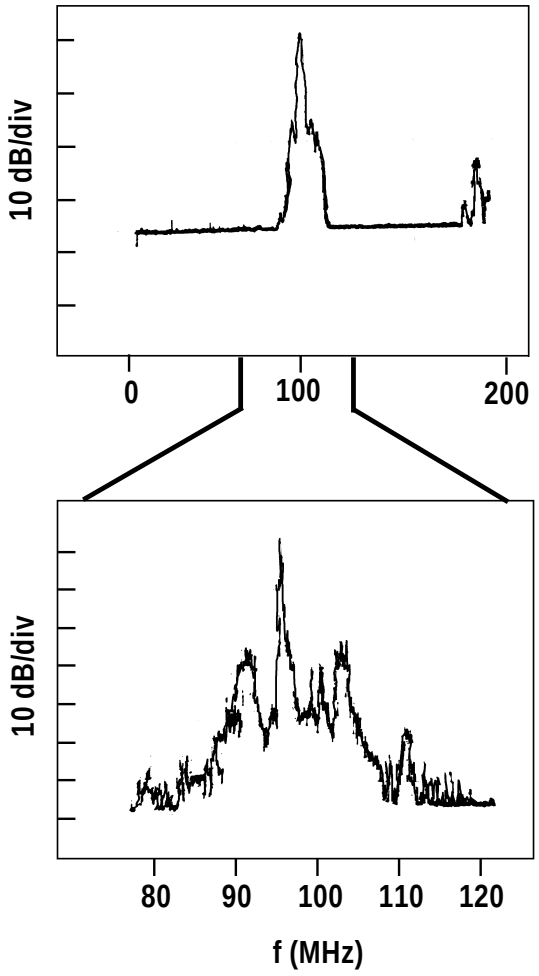

Fig. 8. Spectrum of the low frequency parasitic oscillation after installation of the filter and collar. The center frequency is about 96 MHz and sidebands are visible. The second harmonic is 35 dB below the fundamental.

wings. The FWHM is 14 cm but appreciable power is absorbed within a broader region with 30 cm radius, for absorption centered about 10 cm off the magnetic axis. Fourier analysis of modulated rf injection indicated an even broader power

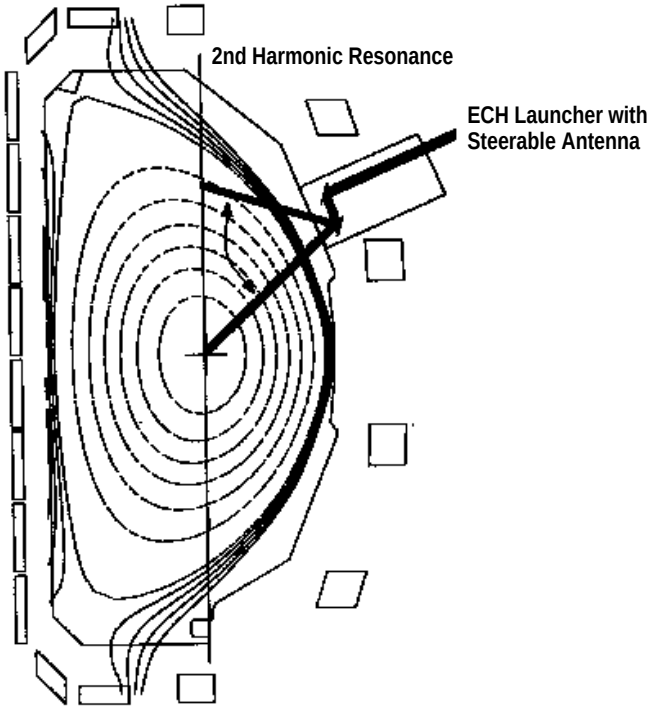

Fig. 9. Cross section of the DIII–D chamber showing the poloidal scan of the injected rf power.

deposition profile. Presently, measurements of the elliptical polarization of the beam launched into DIII–D are being performed under the assumption that an admixture of O–mode is present.

It is characteristic of the operation of this system that there is some reflected power measured at the first miter bend during the first 100 msec of the rf pulse. The forward power measurement has a maximum value during this part of the pulse and then drops, reaching a steady value after about 200 msec. The reflected power decreases to unmeasurable levels after the first 100 msec. An rf monitor on the MOU is also available to indicate the rf power reflecting in the MOU and not a part of the Gaussian beam. These rf monitor traces are shown in Fig. 11, both for an unmodulated and a modulated case. For the modulated case, the high voltage, the collector sweep coil current and the window arc detector

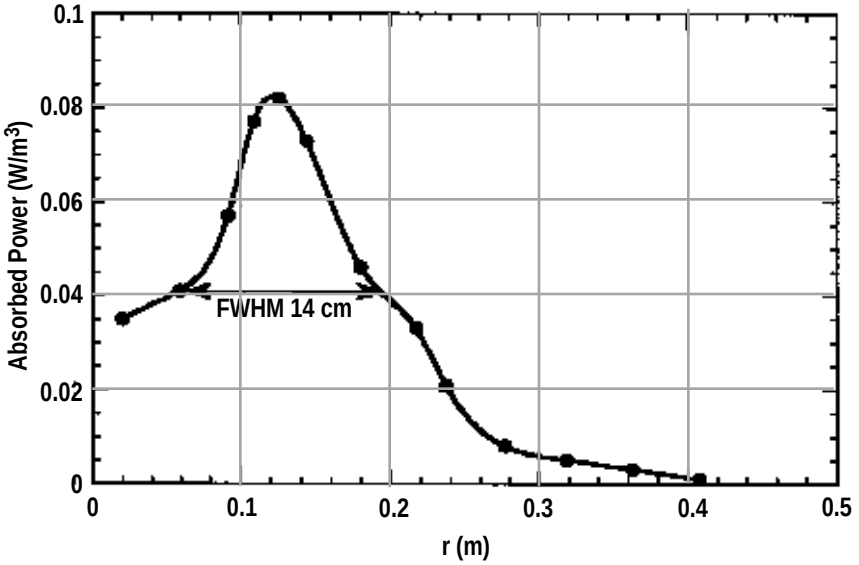

Fig. 10. Power deposition profile measured from the time derivative of the ECE T_e signal upon termination of the rf pulse. The profile is broader than calculated from the optics of the launcher.

signal are also displayed. The beam voltage is modulated approximately 13% to obtain greater than 60% modulation of the generated rf power. These traces were for injection into DIII–D plasmas for the full 500 msec long pulses.

Injection of approximately 500 kW into DIII–D plasmas at low density has resulted in electron temperatures as high as 12 keV. Traces of the discharge with the highest T_e are shown in Fig. 12 along with the electron temperature profile from the Michelson interferometer, the heterodyne radiometer and Thomson scattering. The radiometer data show a suprathermal electron population at these low densities.

VI. CONCLUSION

The Gycom Centaur gyrotron is now running routinely at DIII-D with generated power in all modes at 110 GHz of approximately 900 kW, pulse lengths up to 500 msec and good power accountability. The efficiency is 35% for 110 GHz rf power generation and better than 95% for the evacuated windowless transmission line to the tokamak. Approximately 15%–25% of the power generated by the gyrotron, as inferred from window calorimetry, appears in the MOU.

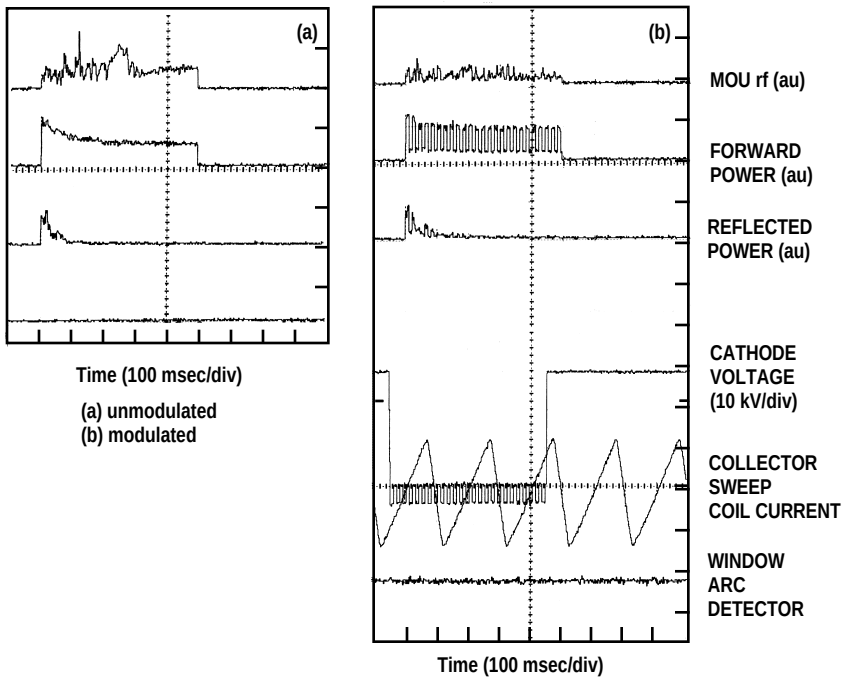

Fig. 11. The rf monitor signals for unmodulated and modulated 500 msec long pulses. The sawtooth signal is the collector sweep coil current. A 13% modulation of the cathode high voltage yields a 60% rf output modulation for transport studies.

Initial injection into DIII–D plasmas has been performed for 500 msec pulses. The MHD measurements of plasma energy indicated that about 550 kW was absorbed in the plasma for about 800 kW generated. Initial transport experiments using modulation of the 110 GHz rf have been performed and ECH synergy for fast wave current drive was investigated.

ACKNOWLEDGMENT

The authors are grateful to Max Austin for providing the T_e profile data and to R.E. Brambila for technical support.

This is a report of work supported by U.S. Department of Energy Contract DE-AC03-89ER51114

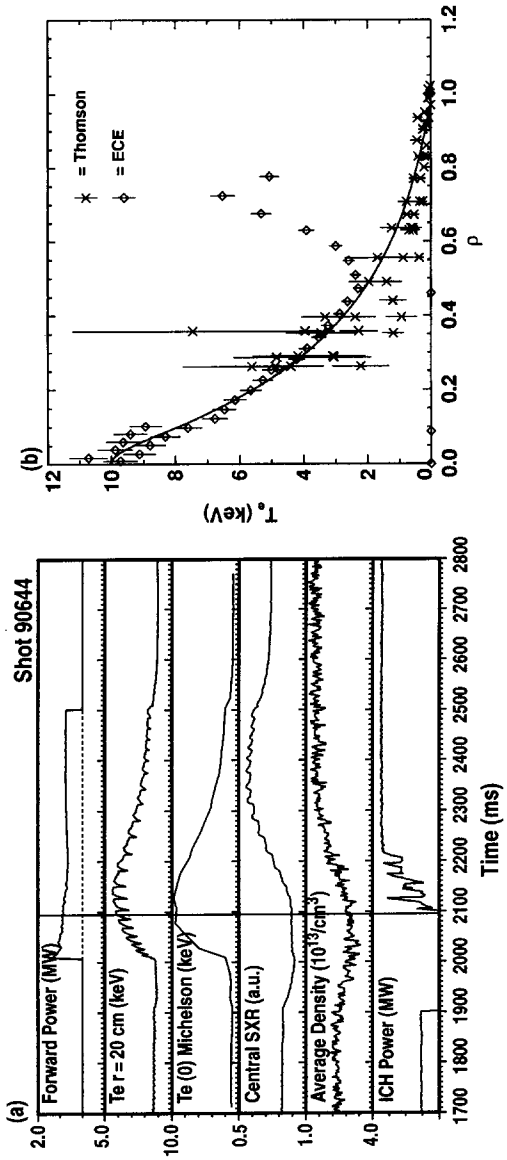

Fig. 12. Time dependence of the forward rf power nd several diagnostic traces during ECH/fast wave synergy experiments: (a) the electron temperature profile (b) from ECE and Thomson scattering is shown at the time indicated by the vertical line on the time plots. The density increase associated with the injection of ICH power at 2100 msec decreases the value. Comparison of the ECE and Thomson data at indicates a superthermal electron velocity distribution function during the low density portion of the discharge.

REFERENCES

1. M.V. Agapova, V.V. Alikaev, L.A. Axenova, *et.al.*, Proc. 20th Int. Conf. on Infrared and Millimeter Waves, Ed. R. Temkin, Coca Beach, Florida, 205, 1995.
2. K. Ohkubo, Proc. U.S./Japan RF Technology Exchange, unpublished (1995).
3. John L. Doane, Infrared and Millimeter Waves, **13**, 123, 1985.
4. H. Stickel, Int. J. Electronics, **64**, 63, 1988.
5. V. Zapevalov, private communication.
6. V.E. Myasnikov *et al.*, these proceedings.